Trends in Computational and Applied Mathematics
Trends in Computational and Applied Mathematics, **27** (2026), e01879
Sociedade Brasileira de Matemática Aplicada e Computacional
Online version ISSN 2676-0029 www.scielo.br/tcam
ORIGINAL ARTICLE
doi: 10.5540/tcam.2026.027.e01879

A Novel Convolutional Neural Network for Semantic Segmentation of Microscopic and Retinal Images

A. L. O. DA SILVA[1*] and W. CASACA[2]

Received on June 26, 2025 / Accepted on August 27, 2026

ABSTRACT. Semantic segmentation of medical images remains a challenging task, particularly for microscopic cell images and retinal fundus photographs, where precise boundary delineation and structural preservation are critical. In this work, we tackle these two applications by proposing a new convolutional neural network based on U-Net with a structured depth schedule that concentrates representational capacity at the lower-resolution bottleneck phases, improving edge definition, region filling and structural detail recovery. Our model was evaluated on two benchmark datasets covering both application domains and compared against six established baselines. For microscopic cell segmentation, it achieved the best scores in PSNR, SSIM, Precision and F1-Score. For retinal vessel extraction, it led in SSIM and Recall while placing second in IoU and F1-Score, presenting the most balanced performance profile among all evaluated models. Qualitative results confirm sharper segmentation boundaries and finer structural details relative to all competing methods, including under challenging illumination and background conditions.

Keywords: semantic segmentation, computer vision, AI.

1 INTRODUCTION

In the field of Computer Vision (CV), new techniques have been successfully developed to address a wide range of real-world challenges, including object detection [17], face detection [23], human face recognition [10], handwritten digit classification [45], garment classification [18] and image inpainting [15]. These CV approaches aim not only to replicate human capabilities but also to exceed them in specific tasks, such as recognizing complex patterns in large-scale datasets.

Among these tasks, semantic segmentation in medical imaging has received particular attention, with Convolutional Neural Network (CNN)-based methods studied extensively over the past two decades. Notable works address a range of problems, including cell segmentation [34], tumors

*Corresponding author: André Luiz Ortiz da Silva – E-mail: andre.silva@ufnt.edu.br
[1] Federal University of Northern Tocantins (UFNT), Centro de Ciências Integradas (CCI), 77824-838, Araguaína, TO, Brazil – E-mail: andre@ufnt.edu.br https://orcid.org/0009-0000-1233-1112
[2] São Paulo State University (UNESP), Institute of Biosciences, Humanities and Exact Sciences (IBILCE), São José do Rio Preto, SP, Brazil – E-mail: wallace.casaca@unesp.br https://orcid.org/0000-0002-1073-9939

[2], polyps [11, 22], retinal structures [1, 5], COVID-19 lesions [6, 39], and the pancreas [32]. This broad applicability highlights the versatility and importance of CNN-based approaches in medical image analysis.

In this study, we focus on microscopic cell images and retinal fundus images, where semantic segmentation faces several open challenges. These challenges involve developing more effective models that can simultaneously address key issues, such as enhancing segmentation quality, increasing pixel overlap with the ground-truth mask and preserving structural integrity. Our goal is to improve region-filling accuracy while maintaining contour sharpness, and to generalize effectively across datasets with varying image sizes.

To jointly address these challenges, we introduce a new convolutional neural network inspired by the U-Net architecture [34], with architectural modifications that improve segmentation accuracy and generalize across two distinct medical imaging tasks: microscopic cell segmentation and retinal vessel extraction.

In summary, the main contributions of this work are:

1. The proposed model yields segmentations that both preserve original structures more effectively and deliver finer pixel-level filling.
2. Our approach improves region-filling accuracy while maintaining contour precision, recovering finer details in segmented images through more balanced feature extraction.
3. Once trained, the segmentation models can be applied directly to analyze both microscopic and retinal images, generalizing effectively across datasets regardless of variations in image type or size.

This work is organized as follows: Section 2 reviews related work, while Section 3 describes the proposed architecture. Section 4 presents the experimental results, Section 5 discusses the findings and Section 6 concludes our study.

2 RELATED WORK

We now present some of the latest research in semantic segmentation, highlighting models that achieve performance close to the state of the art.

Eigen et al. [14] presented a multi-scale neural network called EPF, employing two network stacks: one producing a coarse global prediction from the full image, and another refining it locally, achieving leading performance on the NYU Depth and KITTI datasets. Casaca et al. [7] proposed two segmentation algorithms based on spectral clustering, the Laplacian operator, spectral graph theory, and energy functional minimization, showing superior results in both qualitative and quantitative evaluations. Hatamiza et al. [16] introduced the Edge-Gate (EG) module for CNNs, designed to jointly process edges and textures, which consistently improved segmentation accuracy and generalization when incorporated into multiple architectures and evaluated on brain tumor and kidney segmentation datasets.

Regarding biomedical image segmentation, Ronneberger et al. [34] introduced U-Net, a convolutional neural network designed for microscopic biomedical images that set a new standard for the field. In [12], the authors proposed two networks for segmenting various objects, achieving results close to the state of the art on the PASCAL VOC and PASCAL CONTEXT datasets while maintaining fast computational speed. Similarly, [30] introduced the Fully Convolutional Network (FCN), combining deep semantic features with shallow appearance details to produce accurate dense predictions. The model achieved leading performance on PASCAL VOC, NYUDv2, and SIFT Flow.

The segmentation problem is also central in medical imaging. For instance, Kaylibay et al. [25] introduced KJS, a CNN using three-dimensional filters for hand and brain MRI segmentation, validated on central nervous system and hand bone data, while Jha et al. [22] proposed ResUnet++ for colonoscopy polyp segmentation, outperforming both U-Net and ResUNet, attaining a Dice coefficient of 81.33% on Kvasir-SEG and 79.55% on CVC-612 dataset. Alalwan et al. [2] presented an efficient 3D deep learning model for semantic segmentation of tumor diseases in medical images, achieving highly effective and efficient results compared to related studies, while Chen et al. [9] introduced TransUNet: a hybrid transformer-U-Net model for medical image segmentation that outperformed several methods on multi-organ and cardiac benchmarks. Huo et al. [19] applied the nnU-Net to stroke lesion segmentation, securing first place in the MICCAI 2022 ATLAS Challenge.

Deep learning has been the focus of several studies on microscopic image analysis. Shahzad et al. [36] combined a convolutional encoder-decoder with the popular VGG-16 architecture for pixel-level feature extraction, achieving 97.18% overall accuracy and 91.96% average accuracy. Koohbanani et al. [26] proposed NuClick, an interactive segmentation framework for microscopy that annotates nuclei and cells with a single click, placing first in the LYON19 challenge. Trampert et al. [38] showed that regenerative CNN models outperform random-pixel-selection approaches on microscopic images, while Liu et al. [28] developed an AI-based classification system that achieved 96.83% accuracy and 96.82% F1-Score. Further work in this area includes [20], [33] and [46].

For vessel segmentation analysis and related medical imaging tasks, Ahmed et al. [1] proposed DoubleU-NetPlus, a dual U-Net architecture that obtained Dice scores of 85.17%, 99.34%, 94.30%, 96.40%, 95.76%, and 97.10% on the DRIVE, LUNA, BUSI, CVCclinicDB, 2018 DSB, and ISBI 2012 datasets, respectively. Benvenuto et al. [5] developed an unsupervised deep learning framework for non-rigid retinal fundus image registration, reporting SSIM scores of 0.9338 (Network), 0.8640 (Opening), 0.8625 (Closing), 0.9613 (CCA 10), 0.9611 (CCA 20), and 0.9598 (CCA 30). Related work on this particular field includes [32], [11] and [40]. Chatterjee et al. [8] addressed cerebral blood vessel segmentation from MR angiography, achieving a Dice score of 80.44 ± 0.83 on the test set, while Shah et al. [35] applied U-Net to segment graphene scanning electron microscopy images, finding that smaller high-quality training sets outperform larger low-quality ones.

Lesion and disease segmentation have also received considerable attention. Wu et al. [41] recently developed W-Net, a boundary-enhanced U-Net variant for brain lesion segmentation, showing that the architecture preserves stroke lesion details with competitive performance. Bruzadin et al. [6] proposed a diffusion-based model for segmenting COVID-19 lung CT images, validated against multiple baselines both qualitatively and quantitatively related work on COVID-19 segmentation.

Broader perspectives on semantic segmentation are provided by the surveys of [4], [27], and [43], and by the review on transformer-based architectures for stroke segmentation of [44]. On the methodological side, Xie et al. [42] introduced an adversarial co-training approach for medical image segmentation with improved robustness to distribution shifts [3]. Jeon et al. [21] proposed a multi-organ segmentation network in which part of the encoder spatially distorts abdominal scan data prior to spline-based alignment, improving accuracy, whereas Dumont et al. [13] applied deep learning to telescope image segmentation for phase-error detection, also demonstrating robustness under noise.

For the segmentation and detection of aneurysms, Nader et al. [31] conducted a study using deep neural networks. Their model is designed to mimic various components of the brain and its vascular tree, including cerebral arteries, bifurcations, and intracranial aneurysms, enhancing the accuracy of aneurysm identification. In [29], the authors introduced the Snet neural network for medical image segmentation, particularly for brain imaging. Experimental results demonstrated that Snet outperforms recent segmentation techniques on the Synapse dataset, which contains images of varying sizes.

These studies highlight the wide range of applications for semantic image segmentation across different domains, underscoring the significance of this research field. In the next section, we introduce the proposed model and provide further details on our study.

3 PROPOSED ARCHITECTURE

This section presents the architecture of the proposed convolutional neural network, which is based on the U-Net model [34] but incorporates significant modifications.

The standard U-Net applies a fixed number of two convolutional blocks at every encoder and decoder phase, which distributes feature extraction uniformly regardless of spatial resolution. This can limit the model's ability to capture complex representations at the deeper, lower-resolution phases, where the most semantically rich features are formed. The proposed design addresses this by following a structured depth schedule: the number of convolutional blocks increases gradually in the early encoding phases, remains fixed at three blocks from phases three through seven, and decreases in the final two phases, as illustrated in Figure 1.

The model comprises 73,329,985 parameters (73,313,345 trainable and 16,640 non-trainable) and operates on 256$\times$256 images. Feature extraction is performed at every stage via convolutional layers, combining early and late encoder representations through progressive skip connections [25]. By concentrating deeper feature extraction in the central phases, where spatial

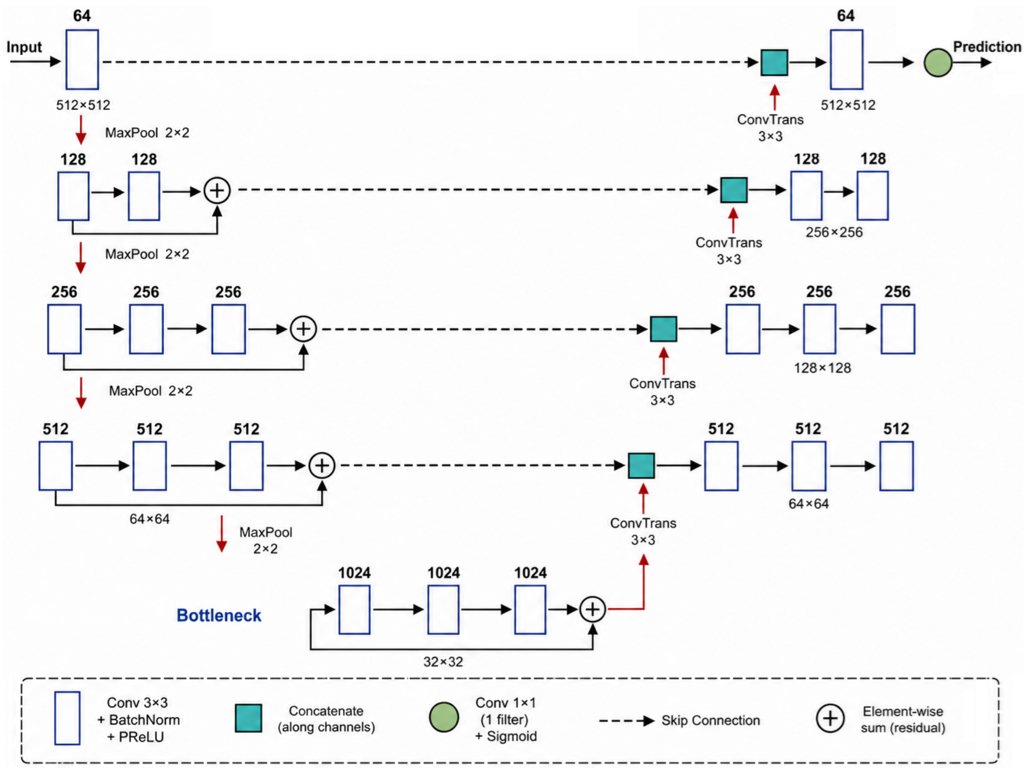

Figure 1: Proposed architecture.

resolution is lowest, the model retains finer structural details and sharper edge definitions in the final segmentation.

The U-Net model represented a significant breakthrough in biomedical image segmentation. However, its architecture standardizes feature extraction with two convolutional blocks across all phases, potentially leading to information loss in lower-resolution stages. To address this, the proposed model concentrates feature extraction in the central phases, where spatial resolution is lowest, yielding finer segmentation details, sharper edge definition, and better structural preservation.

Figure 2 compares the input image, ground-truth mask and predictions from both segmentation models on microscopic images. As observed, the proposed model captures finer cellular details and preserves shapes more accurately than U-Net, producing segmentations closer to the ground truth. Figure 3 shows the corresponding comparison on retinal images. Our approach produces sharper vessel contours and recovers finer vascular structures, with segmentations that more closely follow the ground-truth mask. U-Net, by contrast, exhibits visible segmentation flaws, missing thin vessel branches and producing less precise boundary delineation.

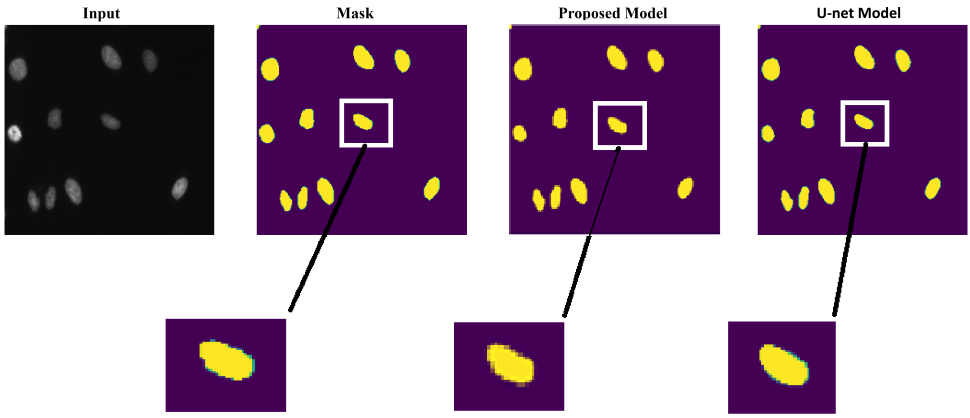

Figure 2: Segmentation comparison: proposed vs. U-Net (microscopic images).

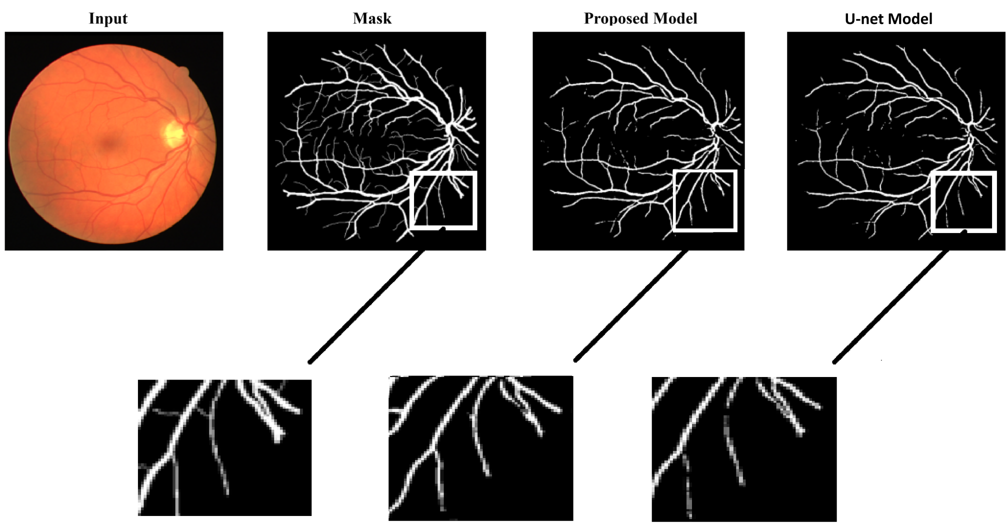

Figure 3: Segmentation comparison: proposed vs. U-Net (retinal images).

4 RESULTS

This section presents the experimental results obtained on the two image benchmarks employed in our analysis.

The first dataset, Data Science Bowl 2018 [24], is a microscopic cell image benchmark comprising 670 images and corresponding segmentation masks, covering a diverse range of cell types and staining conditions. The data was split into 1,206 training, 134 validation, and 65 test images, all resized to 256×256 pixels. Sample images and masks are shown in Figure 4.

The second dataset, DRIVE (Digital Retinal Images for Vessel Extraction) [37], is a retinal fundus image benchmark for vessel segmentation, comprising 20 training images with masks and 40 test images at 512×512 pixels. Representative samples are illustrated in Figure 5. Given the limited training set size, data augmentation was applied to expand it to 120 training and 24 validation images. The augmentation pipeline included random horizontal and vertical flips, rotations in $[-15°, +15°]$, brightness and contrast adjustments, and elastic deformations, following standard practices for retinal vessel segmentation [5].

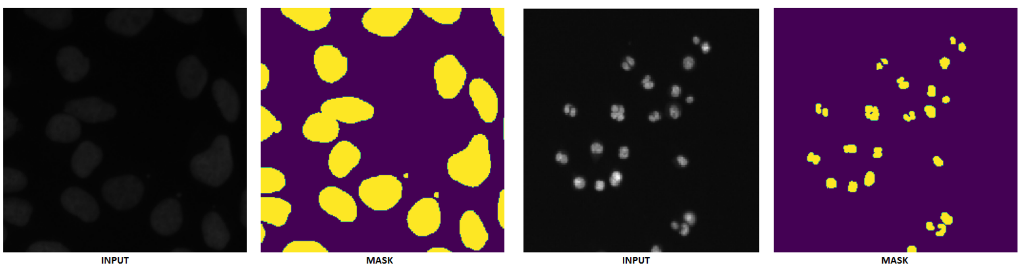

Figure 4: Sample images and masks from the Data Science Bowl 2018 dataset.

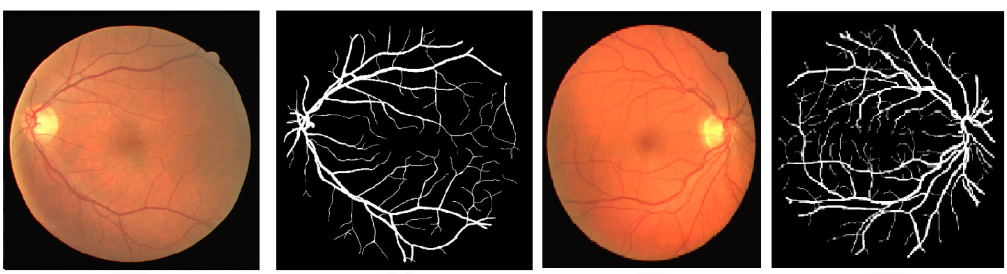

Figure 5: Sample images and masks from the DRIVE dataset.

All models, including the proposed network and other methods, were implemented in Python and trained for 30 epochs on both datasets using Google Colab with a T4 GPU. Performance is assessed through qualitative and quantitative analyses using error rate, accuracy, PSNR, SSIM, IoU, Recall, Precision and F1-score.

4.1 Results on Microscopic Cell Images

Table 1 reports the training and validation error and accuracy for all evaluated models, with bold values indicating the best result in each column. The tabulated scores demonstrate that the proposed model outperformed the other six models, achieving superior accuracy in both training (97.76%) and validation (98.39%), with the lowest training and validation errors of 0.0591 and 0.0430, respectively.

Table 1: Comparison of error rate and accuracy across all evaluated models.

Model	Training error	Training accuracy	Val. error	Val. accuracy
Proposed	**0.0591**	**97.76%**	**0.0430**	**98.39%**
U-Net	0.0712	97.58%	0.0797	97.20%
FCN	0.2039	90.49%	0.1788	91.71%
EPF	0.2792	87.59%	0.3158	86.64%
ResUnet++	0.0628	97.63%	0.0681	97.17%
KJS	0.0691	97.29%	0.0559	97.92%
W-Net	0.0594	97.73%	0.0564	97.88%

Table 2 reports the remaining evaluation metrics for all models. The results show that the proposed model achieves the best scores in PSNR, SSIM, Precision and F1-Score. W-Net obtains the highest IoU (0.9168 vs. 0.9075 for the proposed model) and KJS achieves the best Recall. Overall, the proposed model delivers the strongest combined performance across the majority of metrics, producing segmentations with lower image noise, higher structural similarity, and a better balance between precision and recall.

Table 2: Comparison of performance metrics across all evaluated models.

Model	PSNR	IoU	SSIM	Recall	Precision	F1-Score
Proposed	**67.775**	0.9075	**0.9263**	0.8881	**0.9655**	**0.9252**
U-Net	66.751	0.8850	0.8968	0.8980	0.9296	0.9135
FCN	60.681	0.6364	0.7993	0.5804	0.7266	0.6453
EPF	44.443	0.5710	0.7256	0.4335	0.6425	0.5177
ResUnet++	65.712	0.8838	0.8772	0.9044	0.9184	0.9113
KJS	67.451	0.9076	0.9075	**0.9201**	0.9180	0.9191
W-Net	67.069	**0.9168**	0.8994	0.8939	0.9015	0.8882

Regarding qualitative results, Figure 6 depicts the original images, ground-truth masks and predictions from all segmentation models. Among these, the proposed model, U-Net, KJS and W-Net produced visually similar segmentations, all preserving structural details and closely matching the ground-truth masks. FCN, EPF and ResUnet++, by contrast, produced notably inferior outputs.

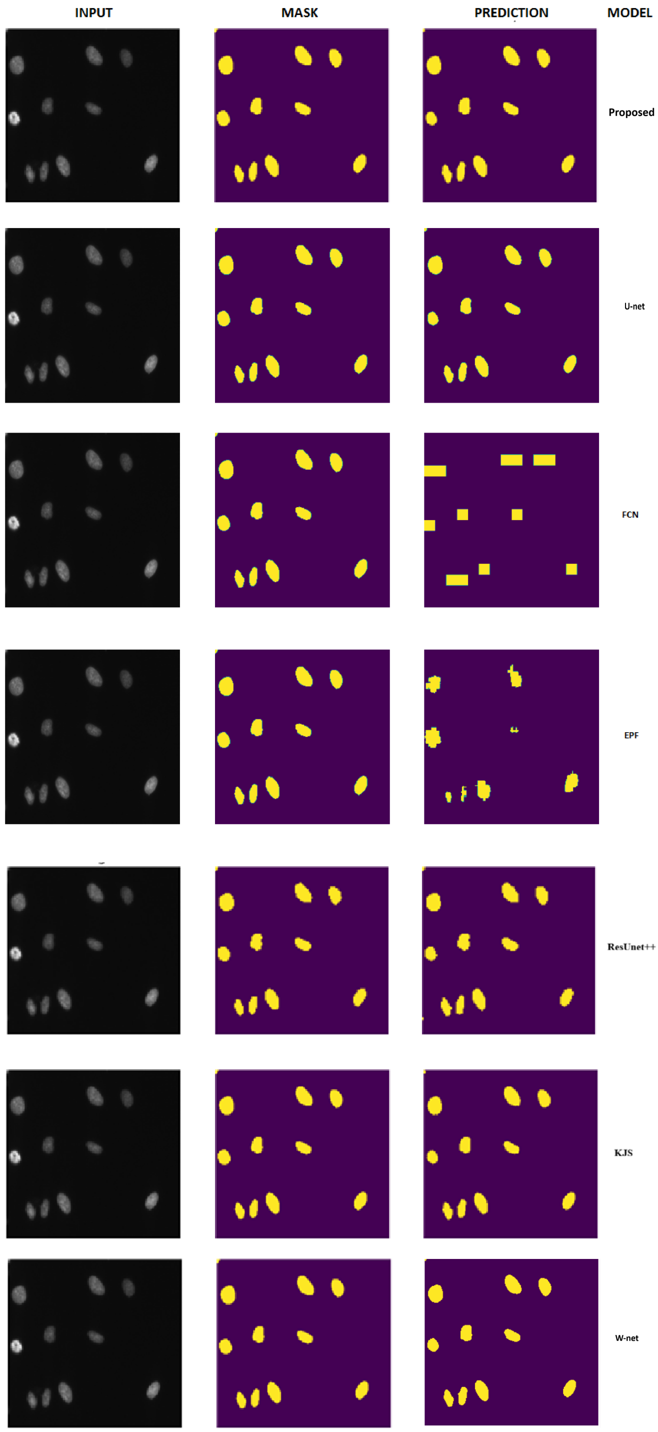

Figure 6: Visual comparison of segmentations across all evaluated model.

Figure 7 shows prediction outputs for various microscopic image types drawn from the test set. The proposed model maintains accurate segmentation across images with different background colors: an additional challenge that typically degrades segmentation performance. Despite this variability, the predictions retain fine structural details and well-defined region boundaries, which can directly support downstream tasks such as cell classification and clinical diagnosis.

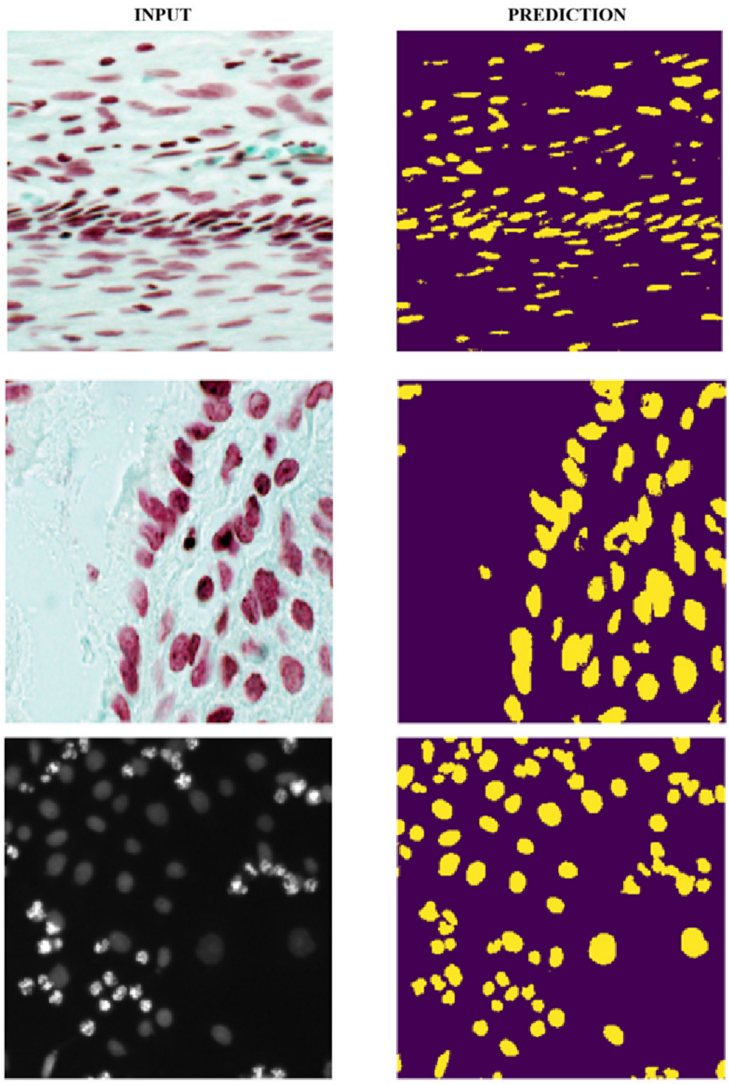

Figure 7: Segmentation results of the proposed model on microscopic test images.

4.2 Results on Retinal Fundus Images

Table 3 reports the training and validation error and accuracy for all evaluated models on the DRIVE dataset, with bold values indicating the best result in each column. The proposed model achieves the best validation accuracy (91.71%) and the lowest validation error (0.1203), reflecting strong generalization to unseen retinal images. W-Net, in turn, obtains the lowest training error (0.0655) and the highest training accuracy (92.98%), indicating effective fitting on the training set.

Table 3: Comparison of error rate and accuracy across all evaluated models.

Model	Training error	Training accuracy	Val. error	Val. accuracy
Proposed	0.0897	92.59%	**0.1203**	**91.71%**
U-Net	0.1039	92.41%	0.1221	91.70%
FCN	0.2765	87.60%	0.2721	87.70%
EPF	0.2596	87.63%	0.2553	87.72%
ResUnet++	0.1598	91.69%	0.2330	90.13%
KJS	0.0898	92.53%	0.1274	91.43%
W-Net	**0.0655**	**92.98%**	0.1264	91.61%

In Table 4, we detail the performance metrics obtained for all segmentation models. The results indicate that the proposed model achieves the best SSIM and Recall scores. W-Net obtains the highest PSNR (63.088), while KJS achieves the highest IoU (0.8208 vs. 0.7587 for ours), as well as superior Precision and F1-Score. Despite not leading in every metric, the proposed model ranks second in IoU and F1-Score, remaining competitive across all metrics while leading in those most directly related to structural preservation and vessel recovery.

Table 4: Comparison of performance metrics across all evaluated models.

Model	PSNR	IoU	SSIM	Recall	Precision	F1-Score
Proposed	56.956	0.7587	**0.7631**	**0.8751**	0.7066	0.7819
U-Net	19.975	0.6086	0.7598	0.2748	0.9065	0.4217
FCN	59.299	0.4734	0.6781	0.0000	0.0000	0.0000
EPF	59.196	0.4674	0.6779	0.0697	0.4839	0.1218
ResUnet++	61.134	0.6932	0.5140	0.6695	0.5096	0.5787
KJS	57.422	**0.8208**	0.7630	0.7850	**0.8189**	**0.8016**
W-Net	**63.088**	0.7560	0.7087	0.6715	0.8098	0.7342

Figure 8 shows the original retinal images, ground-truth masks and predictions from all evaluated models. The proposed model, U-Net and KJS produced visually similar segmentations, but upon closer inspection against the ground-truth masks, the proposed model exhibits greater sharpness and finer vessel details. ResUnet++, FCN, and EPF did not produce satisfactory predictions for

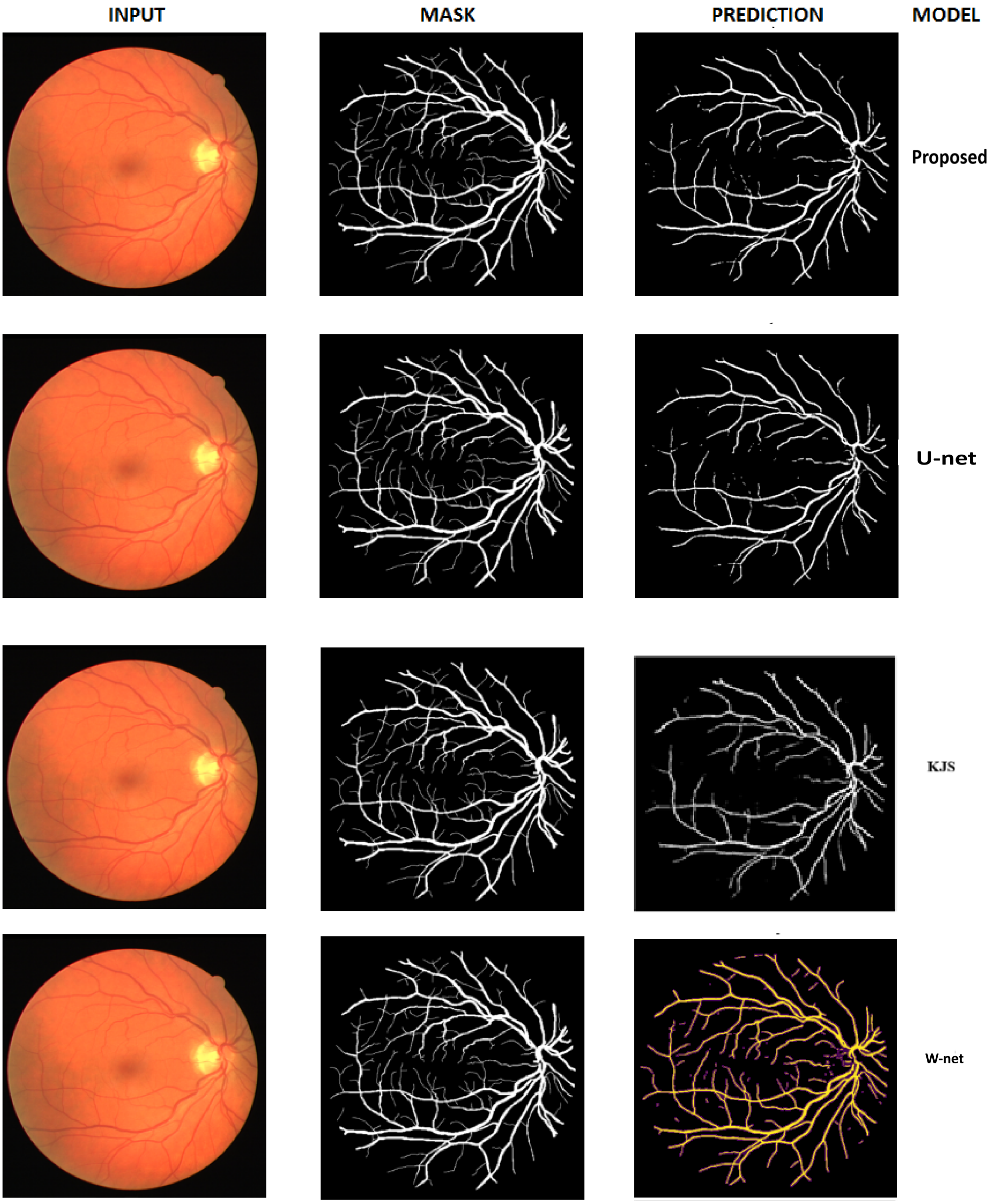

Figure 8: Visual comparison of segmentations across all evaluated model.

this image, while W-Net generated a non-binary output, failing to produce a proper segmentation mask.

Figure 9 presents retinal test images captured under varying lighting conditions, along with the corresponding predictions generated by the proposed model. Low illumination is a well-known challenge in retinal vessel segmentation, as it reduces contrast between vessels and background, making precise boundary delineation significantly harder. Despite this, the proposed model consistently produces well-defined segmentations, preserving fine vascular structures and maintaining sharpness and visual clarity across all lighting conditions, which reflects its robustness when applied to images acquired under non-standardized clinical settings.

5 DISCUSSION

This work addressed the semantic segmentation of microscopic cell and retinal fundus images, roposing a U-Net-based architecture with targeted modifications to the depth schedule of convolutional blocks. The structural changes concentrate feature extraction in the lower-resolution central phases, which proved effective in preserving finer structural details and producing sharper segmentation boundaries.

For the microscopic images in the Data Science Bowl 2018 dataset, the proposed model achieved the lowest errors, the highest accuracies and the best scores for PSNR, SSIM, Precision, and F1-Score. W-net obtained the highest IoU. while KJS achieved the best Recall. Nevertheless, the proposed model delivers superior overall performance across the majority of metrics, producing higher-quality images with better-defined structures compared to the other models.

Turning to the retinal images in the DRIVE dataset, the proposed model achieved the best validation accuracy and validation error, along with the best SSIM and Recall scores, and the second-best IoU and F1-score. W-Net led in training accuracy and training error, and obtained the highest PSNR. KJS obtained higher IoU, Precision, and F1-Score values. Notwithstanding, the proposed model fills the segmented regions more efficiently and preserves finer vessel contours with greater precision, as evidenced by the qualitative results.

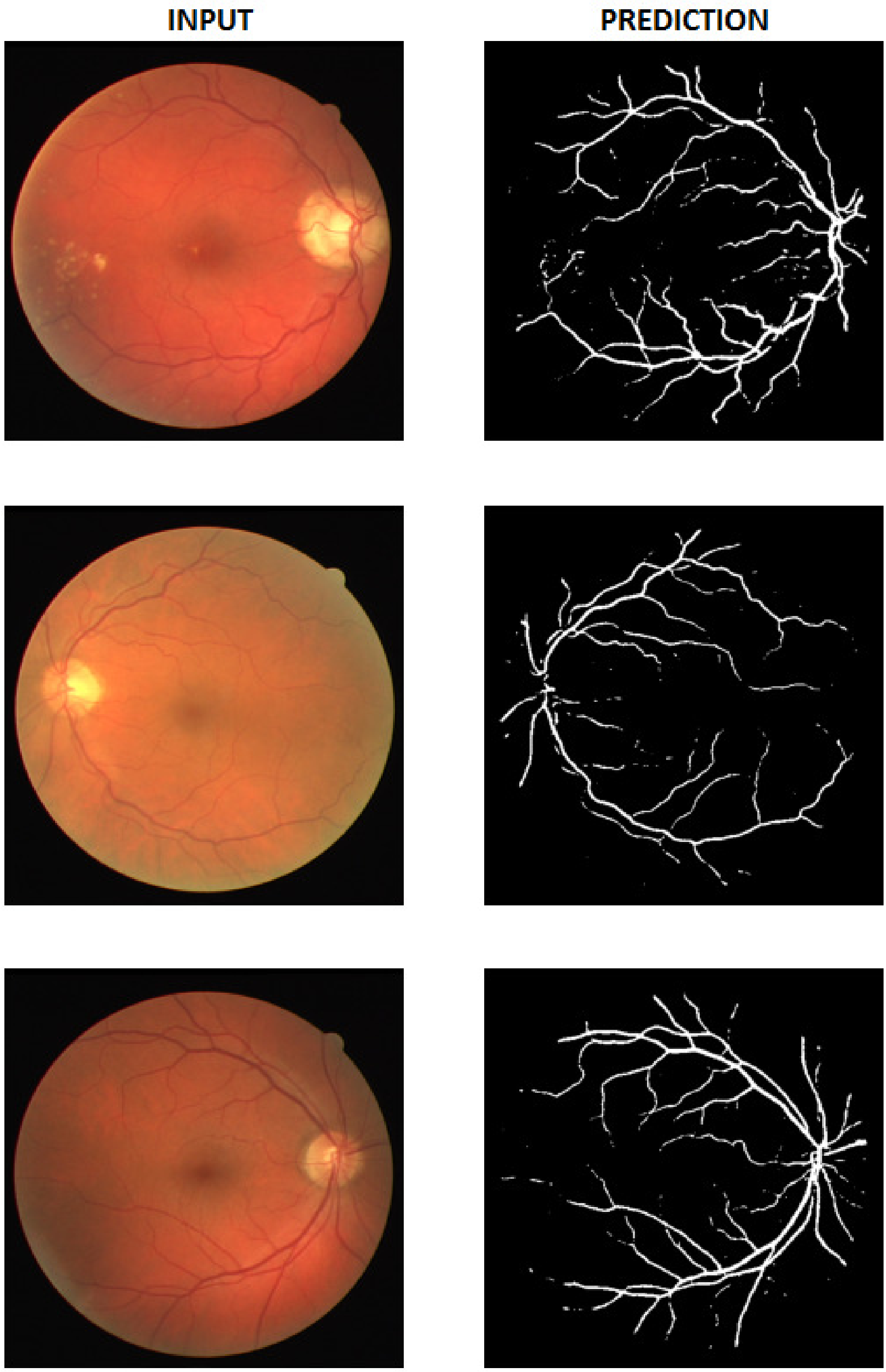

Figure 9: Segmentation results of the proposed model on retinal test images.

6 CONCLUSION

This work introduced a U-Net-based convolutional neural network with a structured depth schedule that concentrates feature extraction in the lower-resolution central phases of the encoder. Experiments on two benchmark datasets, including microscopic cell images from the Data Science Bowl 2018 and retinal fundus images from DRIVE, showed that the proposed model achieves competitive or superior performance relative to five established baselines, leading in SSIM and Recall across both tasks and presenting a consistently balanced profile across all evaluated metrics.

The key architectural contribution lies in replacing U-Net's uniform two-block scheme with a variable-depth design that allocates more representational capacity where it is most needed: at the bottleneck phases where spatial resolution is lowest and semantic content is richest. This design choice translates into finer structural details, sharper edge definitions, and more accurate region filling in the final segmentation outputs.

For future work, we aim to extend the application of the proposed model to additional datasets, particularly medical images of human organs, to further evaluate its performance and explore potential contributions of this novel convolutional neural network.

Funding

We acknowledge FAPESP (#2024/04492-0) for financial support.

Data availability

All data generated or analysed during this study are included in this published article.

Associate editor: Paulo Pagliosa

REFERENCES

[1] M.R. Ahmed, A.F. Ashrafi, R.U. Ahmed, S. Shatabda, A.K.M.M. Islam & S. Islam. DoubleU-NetPlus: a novel attention and context-guided dual U-Net with multi-scale residual feature fusion network for semantic segmentation of medical images. *Neural Computing and Applications*, **35**(19) (2023), 14379–14401. doi:10.1007/s00521-023-08493-1.

[2] N. Alalwan, A. Abozeid, A.A. ElHabshy & A. Alzahrani. Efficient 3D Deep Learning Model for Medical Image Semantic Segmentation. *Alexandria Engineering Journal*, (60) (2021), 1231–1239.

[3] S. Asgari Taghanaki, K. Abhishek, J.P. Cohen & et al. Deep semantic segmentation of natural and medical images: a review. *Artificial Intelligence Review*, (54) (2021), 137–178.

[4] R. Azad, E.K. Aghdam, A. Rauland, Y. Jia, A.H. Avval, A. Bozorgpour, S. Karimijafarbigloo, J.P. Cohen, E. Adeli & D. Merhof. Medical Image Segmentation Review: The Success of U-Net. *IEEE*

Transactions on Pattern Analysis and Machine Intelligence, **46** (2024), 10076–10095. doi:10.1109/TPAMI.2024.3435571.

[5] G.A. Benvenuto, M. Colnago, M.A. Dias, R.G. Negri, E.A. Silva & W. Casaca. A fully unsupervised deep learning framework for non-rigid fundus image registration. *Bioengineering*, **9**(8) (2022), 369.

[6] A. Bruzadin, M. Boaventura, M. Colnago, R.G. Negri & W. Casaca. Learning label diffusion maps for semi-automatic segmentation of lung CT images with COVID-19. *Neurocomputing*, (522) (2023), 24–38.

[7] W.C.O. Casaca. "Graph Laplacian for spectral clustering and seeded image segmentation". Ph.D. thesis, ICMC, Universidade de São Paulo, São Carlos, SP (2015).

[8] S. Chatterjee, K. Prabhu, M. Pattadkal, G. Bortsova, C. Sarasaen, F. Dubost, H. Mattern, M. de Bruijne, O. Speck & A. Nürnberger. Deformation-Aware Semi-Supervised Learning: Application to Small Vessel Segmentation with Noisy Training Data. *Imaging*, **8**(259) (2021), 1–22.

[9] J. Chen, Y. Lu, Q. Yu, X. Luo, E. Adeli, Y. Wang, Le Lu, A.L. Yuille & Y. Zhou. TransUNet: Transformers Make Strong Encoders for Medical Image Segmentation (2021). Preprint at `https://arxiv.org/abs/2102.04306v1`.

[10] J. Chen, X. Yang, Y. Dong, H. Su, J. Peng & Z. Yin. FaceCat: Enhancing Face Recognition Security with a Unified Generative Model Framework (2024). Preprint at `https://arxiv.org/abs/2403.18186v1`.

[11] Z. Cheng, A. Qu & X. He. Contour-aware semantic segmentation network with spatial attention mechanism for medical image. *Visual Computer*, (38) (2021), 1–31.

[12] J. Dai, K. He & J. Sun. Convolutional Feature Masking for Joint Object and Stuff Segmentation. In "Proceedings of the IEEE Conference on Computer Vision and Pattern Recognition (CVPR)" (2015), p. 3992–4000. doi:10.1109/CVPR.2015.7299025.

[13] M. Dumont, C.M. Correia, J.F. Sauvage, N. Schwartz, M. Gray & J. Cardoso. Phasing segmented telescopes via deep learning methods: application to a deployable CubeSat (2024). Preprint at `https://arxiv.org/abs/2403.18712v1`.

[14] D. Eigen, C. Puhrsch & R. Fergus. Depth Map Prediction from a Single Image using a Multi-Scale Deep Network. In "Advances in Neural Information Processing Systems (NeurIPS)", volume 27 (2014), p. 2366–2374.

[15] Z. Guo, Z. Chen, T. Yu, J. Chen & S. Liu. Progressive Image Inpainting with Full-Resolution Residual Network. In "Proceedings of the 27th ACM International Conference on Multimedia (MM)" (2019), p. 2496–2504. doi:10.1145/3343031.3351022.

[16] A. Hatamizadeh, D. Terzopoulos & A. Myronenko. Edge-Gated CNNs for Volumetric Semantic Segmentation of Medical Images (2020). Preprint at `https://arxiv.org/abs/2002.04207v1`.

[17] K. He, G. Gkioxari, P. Dollár & R. Girshick. Mask R-CNN. In "Proceedings of the IEEE International Conference on Computer Vision (ICCV)" (2017), p. 2961–2969. doi:10.1109/ICCV.2017.322.

[18] A.S. Henrique, A.M.R. Fernandes, R. Lyra, V.R.Q. Leithardt, S.D. Correia, P. Crocker & R.L.S. Dazzi. Classifying Garments from Fashion-MNIST Dataset Through CNNs. *Advances in Science, Technology and Engineering Systems Journal*, **6**(1) (2021), 989–994.

[19] J. Huo, L. Chen, Y. Liu, M. Boels, A. Granados, S. Ourselin & R. Sparks. MAPPING: Model Average with Post-processing for Stroke Lesion Segmentation (2022). Preprint at `https://arxiv.org/abs/2211.15486v1`.

[20] J. Isaksson, I. Arvidsson, K. Åström & A. Heyden. Semantic segmentation of microscopic images of H&E stained prostatic tissue using CNN. In "International Joint Conference on Neural Networks (IJCNN)" (2017), p. 1252–1256. doi:10.1109/IJCNN.2017.7965996.

[21] Y.S. Jeon, H. Yang, H. Fu & M. Feng. AIC-UNet: Anatomy-informed Cascaded UNet for Robust Multi-Organ Segmentation (2024). Preprint at `https://arxiv.org/abs/2403.18878v1`.

[22] D. Jha, P.H. Smedsrud, M.A. Riegler, D. Johansen, T. de Lange, P. Halvorsen & H.D. Johansen. ResUNet++: An Advanced Architecture for Medical Image Segmentation. In "2019 IEEE International Symposium on Multimedia (ISM)". IEEE (2019), p. 225–2255. doi:10.1109/ISM46123.2019.00049.

[23] V.K. Kadam & D.G. Ganakwar. Face Detection: A Literature Review. *International Journal of Innovative Research in Science, Engineering and Technology*, **6**(7) (2017), 13017–13023.

[24] Kaggle. 2018 Data Science Bowl. `https://www.kaggle.com/c/data-science-bowl-2018` (2018). Accessed: September 2024.

[25] B. Kayalibay, G. Jensen & P. van der Smagt. CNN-based Segmentation of Medical Imaging Data (2017). Preprint at `https://arxiv.org/abs/1701.03056v2`.

[26] N.A. Koohbanani, M. Jahanifar, N.Z. Tajadin & N. Rajpoot. NuClick: A Deep Learning Framework for Interactive Segmentation of Microscopy Images. *Medical Image Analysis*, **65** (2020), 101771. doi:10.1016/j.media.2020.101771.

[27] M. Krithika alias AnbuDevi & K. Suganthi. Review of Semantic Segmentation of Medical Images Using Modified Architectures of UNET. *Diagnostics*, **12**(3064) (2022), 1–31.

[28] R. Liu, W. Dai, T. Wu, M. Wang, S. Wan & J. Liu. AIMIC: Deep Learning for Microscopic Image Classification. *Computer Methods and Programs in Biomedicine*, (226) (2022), 1–12.

[29] T. Liu, Z. Tan, K. Huang & H. Jiang. Rethinking Information Loss in Medical Image Segmentation with Various-sized Targets (2024). Preprint at `https://arxiv.org/abs/2403.19177v1`.

[30] J. Long, E. Shelhamer & T. Darrell. Learning Deconvolution Network for Semantic Segmentation. In "Proceedings of the IEEE International Conference on Computer Vision (ICCV)" (2015), p. 1520–1528.

[31] R. Nader, F. Autrusseau, V. L'Allinec & R. Bourcier. A vascular synthetic model for improved aneurysm segmentation and detection via Deep Neural Networks (2024). Preprint at `https://arxiv.org/abs/2403.18734v1`.

[32] O. Oktay, J. Schlemper, L. Le Folgoc, M. Lee, M. Heinrich, K. Misawa, K. Mori, S. McDonagh, N.Y. Hammerla, B. Kainz, B. Glocker & D. Rueckert. Attention U-Net: Learning Where to Look for the Pancreas. In "1st Conference on Medical Imaging with Deep Learning (MIDL)" (2018). OpenReview: `https://openreview.net/forum?id=Skft7cijM`.

[33] S. Öztürk & B. Akdemir. A convolutional neural network model for semantic segmentation of mitotic events in microscopy images. *Neural Computing and Applications*, (31) (2019), 3719–3728.

[34] O. Ronneberger, P. Fischer & T. Brox. U-Net: Convolutional Networks for Biomedical Image Segmentation. In "Medical Image Computing and Computer-Assisted Intervention (MICCAI)", volume 9351 of *Lecture Notes in Computer Science*. Springer (2015), p. 234–241. doi:10.1007/978-3-319-24574-4_28.

[35] A. Shah, J.A. Schiller, I. Ramos, J. Serrano, D.K. Adams, S. Tawfick & E. Ertekin. Automated image segmentation of scanning electron microscopy images of graphene using U-Net Neural Network. *Materials Today Communications*, (35) (2023), 1–10.

[36] M. Shahzad, A.I. Umar, M.A. Khan, S.H. Shirazi, Z. Khan & W. Yousaf. Robust Method for Semantic Segmentation of Whole-Slide Blood Cell Microscopic Images. *Computational and Mathematical Methods in Medicine*, (2020), 1–13.

[37] J. Staal, M.D. Abràmoff, M. Niemeijer, M.A. Viergever & B. van Ginneken. Ridge-based vessel segmentation in color images of the retina. *IEEE Transactions on Medical Imaging*, **23**(4) (2004), 501–509. doi:10.1109/TMI.2004.825627.

[38] P. Trampert, D. Rubinstein, F. Boughorbel, C. Schlinkmann, M. Luschkova, P. Slusallek, T. Dahmen & S. Sandfeld. Deep Neural Networks for Analysis of Microscopy Images—Synthetic Data Generation and Adaptive Sampling. *Crystals*, **11**(228) (2021), 1–13.

[39] A. Valizadeh & M. Shariatee. The Progress of Medical Image Semantic Segmentation Methods for Application in COVID-19 Detection. *Computational Intelligence and Neuroscience*, (2021), 1–26.

[40] S. Wang, Y. Chen & Z. Yi. nmODE-Unet: A Novel Network for Semantic Segmentation of Medical Images. *Applied Sciences*, **14**(411) (2024), 1–12.

[41] Z. Wu, X. Zhang, F. Li, S. Wang, L. Huang & J. Li. W-Net: A boundary-enhanced segmentation network for stroke lesions. *Expert Systems with Applications*, **230** (2023), 120637.

[42] H. Xie, C. Fu, X. Zheng, Y. Zheng, C.W. Sham & X. Wang. Adversarial co-training for semantic segmentation over medical images. *Computers in Biology and Medicine*, (157) (2023), 1–10.

[43] B. Yuan & D. Zhao. A Survey on Continual Semantic Segmentation: Theory, Challenge, Method and Application. *IEEE Transactions on Pattern Analysis and Machine Intelligence*, **46**(12) (2024), 10891–10910. doi:10.1109/TPAMI.2024.3446949.

[44] Y. Zafari-Ghadim, E.A. Rashed & M. Mabrok. Transformers-based architectures for stroke segmentation: A review (2024). Preprint at `https://arxiv.org/abs/2403.18637v1`.

[45] Z. Zhang, M. Zhou, K. Niu & C. Abdallah. The Effect of Training Parameters and Mechanisms on Decentralized Federated Learning Based on MNIST Dataset (2021). Preprint at `https://arxiv.org/abs/2108.03508v1`.

[46] L. Zhong, L. Li & G. Yang. Benchmarking robustness of deep neural networks in semantic segmentation of fluorescence microscopy images. *BMC Bioinformatics*, **25** (2024), 269.

How to cite

A.L.O. da Silva & W. Casaca. A Novel Convolutional Neural Network for Semantic Segmentation of Microscopic and Retinal Images. *Trends in Computational and Applied Mathematics*, **27**(2026), e01879. doi: 10.5540/tcam.2026.027.e01879.

CC BY